Thermal Conduction in Graphite Flake-Epoxy Composites using Infrared Microscopy

Rajath Kantharaj[1], Ishan Srivastava[1], Kunal R. Thaker[1], Aalok U. Gaitonde[1], Alexandra Bruce[2], John Howarter[2], Timothy S. Fisher[1], Amy M. Marconnet[1]

[1]Birck Nanotechnology Center and School of Mechanical Engineering, Purdue University, West Lafayette, IN 47907, USA
[2]School of Materials Engineering, Neil Armstrong Hall of Engineering, Purdue University, West Lafayette, IN 47907, USA

Email: amarconn@purdue.edu, rkanthar@purdue.edu

ABSTRACT:

Thermally conductive polymer composites, in particular those composed of polymers and carbon-based nanomaterials, are promising for thermal management in electronic devices because they offer high thermal conductivity at low filler loading. The effective thermal properties of these composites exhibit high variability that depend on the topological arrangements and morphological characteristics of the filler particles. In order to tailor the thermal conduction within these composites for use as an efficient heat dissipation material, careful control of the microstructural arrangement of the filler material is required. In this work, we use infrared (IR) microscopy to characterize thermal transport through epoxy composites containing sub-millimeter sized graphitic flakes as filler particles. Graphite flake-epoxy composites of two volume fractions ($3\%, 25\%$) are prepared and characterized using an infrared microscope with a temperature resolution of 0.1 K that images the temperature distribution at the top surface of the composite subject to a temperature gradient. The effective thermal conductivity of the composite with a 25% filler fraction was found to be 2.9 W/m-K, a factor of 16 higher than the neat epoxy. With the micron-scale resolution of the IR microscope, the steady-state particle-scale temperature fields within the composite are directly observed and highlight the non-uniform heat transfer pathways. This local temperature analysis reveals the impact of important microstructural features such as clustering of filler particles. Ultimately, this approach could be used to investigate percolation and anisotropic heat conduction in composites with shear aligned particles.

KEY WORDS: Infrared (IR) microscopy, Thermal conductivity, Percolation, Carbon-based composites

NOMENCLATURE

T	temperature, K
k	thermal conductivity, W/m-K
q''	heat flux, $\mathrm{W/m^2}$
x	thickness, m

Subscripts

c	composite material
eff	effective
ref	reference layer

INTRODUCTION

Increasing functionality and decreasing size of electronic devices have led to an increase in power density. Generated heat must be dissipated efficiently to avoid thermal breakdown of such devices. Graphene nanoplatelet-epoxy composites are potential candidates for thermal interface and packaging materials in high-power devices. High bulk thermal conductivity of graphene nanoplatelet-epoxy or graphene nanoplatelet-polymer composites compared to the matrix phase thermal conductivity has been reported in prior literature [1,2,3]. In addition to the particle and matrix thermal conductivities, the filler particle loading, morphology, topology, and interparticle connectivity are crucial to determining the effective thermal properties of such composites and these topics form the basis of the present study.

Graphene has high thermal conductivity [6], and molecular dynamics simulations have shown that both in-plane and cross-plane thermal conductivities of graphene sheets are governed by the number of layers and lateral size of graphene sheets [2]. In particular, aligning the filler particles can greatly increase thermal conductivity [1]. At low loading fractions of filler particles, interparticle connectivity determines thermal conduction pathways, thereby controlling the bulk thermal conductivity of the composite. Chains of particles form a network across the bulk of the epoxy leading to percolation and typically a significant increase in thermal conductivity. Dispersion, lateral size, and thickness of filler particles are shown to exhibit a strong influence on the thermal conductivity of graphene nanoplatelet-polymer composites at a given loading [3,4,5]. For instance, the effective thermal conductivity of graphene-nanoplatelet composites improved with increasing lateral size and thickness of the nanoplatelets [7], where the effects of dispersion and surface chemistry of filler particles were minimal. In another study, a dry, *in situ* polymerization technique resulted in excellent dispersion of filler particles of varying shapes and sizes, and the associated theoretical models that incorporated waviness of the graphene nanoplatelets yielded better agreement with experimentally characterized thermal conductivity [8]. With increasing aspect ratio of filler particles, the thermal conductivity of graphene nanoplatelet-epoxy composites first increases and then saturates [9].

In spite of many prior computational [10,11,12] and experimental studies [1,3], direct observation of heat conduction pathways that could identify percolating networks of filler particles in such composites is lacking. In addition to percolating contact networks of filler particles, contact topology with higher order contacts between particles is also crucial for enhanced thermal conduction. Three-dimensional microstructure reconstruction techniques [13,14] can potentially help in quantifying contact topology of filler particles in the composite material. This work presents a step toward a correlation between microstructure and transport properties of the composite. Specifically, in this study, we

explore a technique that enables characterization of thermal conductivity of graphite flake-epoxy composites and direct observation of heat conduction pathways. In particular, we use infrared microscopy to observe thermal gradients, heat conduction pathways, and to quantify the thermal conductivity of graphite flake-epoxy composites. Due to the minimum spatial resolution of the microscope (≈ 1.8 μm), we measure thermal transport in composites fabricated with sub-millimeter graphite flakes, rather than true graphene nanoplatelets. Ultimately, this approach enables interrogation of thermal percolation of filler particles, evaluation of composite processing techniques, and begins to evaluate the correlation between microstructure and thermal conductivity. Such a technique is crucial for correlating microstructural signatures with thermal conduction performance.

MATERIALS AND METHODS

MATERIALS

The epoxy prepolymer, EPON 825, was purchased from Hexion LLC (Batesville, AR) with an average molecular weight per epoxide of 175 – 180 g/mol eq. The amine hardener, triethylenetetramine (TETA), was purchased from Sigma-Aldrich Corporation (St. Louis, MO). Graphite flakes were obtained from Asbury Carbons (Asbury, NJ). The particle size distribution was analyzed by Asbury Carbons using a laser particle size analyzer and the median particle diameter is 675 μm. 78.64% of the flakes have a diameter greater than 500 μm; only 6.13% of the flakes are larger than 850 μm (per the technical data sheet by Asbury Carbons). Figure 1 shows SEM micrographs of the graphite flakes. The average thickness of the particles is 20 μm, with a significant variation in thickness (from 6 to 30 μm). The mean aspect ratio is estimated to be 33 based on the median diameter and average thickness. All materials were used as received.

To form composites, the epoxy pre-polymer and graphite flakes were added to a mixing cup in an appropriate ratio, stirred by hand, and then mixed in a Flacktek SpeedMixer™ (model DAC 400) for 1.5 minutes at 2500 rpm. The mixtures were briefly heated for approximately five minutes at 60°C in an oven to reduce the viscosity, and then mixed for an additional 30 seconds at 2500 rpm in the SpeedMixer™. The amine hardener was then added to the epoxy pre-polymer in a 1:1 epoxy-to-amine equivalent ratio (100g: 13.7g by weight), briefly stirred by hand, and mixed for 30 seconds at 2500 rpm in the SpeedMixer, at which point air bubbles visibly disappeared in the mixtures. The mixtures were poured into silicone molds, covered, and allowed to cure at room temperature overnight. The samples were then cured for 2 hours at 100°C followed by 2 hours at 120°C, then allowed to cool to room temperature. Samples were polished flat for thermal characterization. Unfilled epoxy control samples were made following the same procedure without any added graphite.

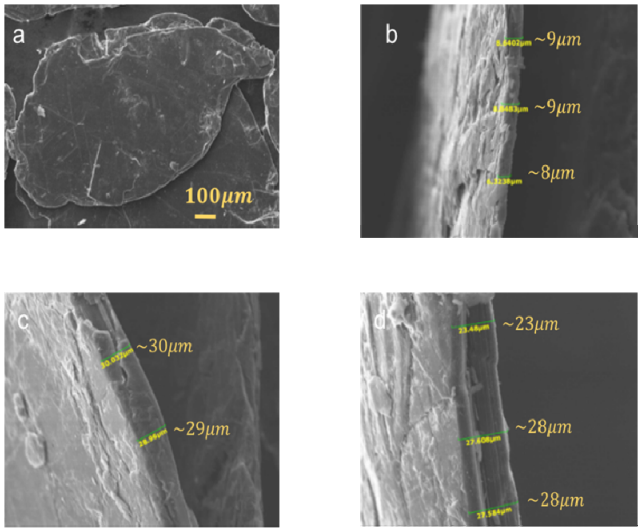

Fig. 1: Example SEM micrographs of graphite flakes. (a) Top view of a particle showing surface irregularities in a particle, (b-d) Cross-sections of the particles indicating significant variation in thickness of the graphite flakes. *(Images courtesy of Asbury Carbons.)*

MINIATURIZED 1D REFERENCE BAR METHOD

The measurement technique here is adapted from the ASTM D5470-12 standard for measuring the thermal conductivity of thermally conductive and electrically insulating materials [15], as in our previous work [16,17]. The major improvement is the integration of infrared microscopy for mapping spatio-temporally varying temperatures with high resolution (see Figure 2), which enables a significant reduction in the size of the sample and experimental rig. Specifically, in this technique, a sample material with unknown thermal conductivity is placed in between reference materials whose thermal conductivity is known; we refer to the arrangement of reference-sample-reference layers as the specimen in this paper. Here, the thermal conductivity of the reference materials (fused silica and polytetrafluoroethylene) has been previously characterized using NIST certified materials (gum rubber [16]).

A temperature gradient is established across the specimen by heating one side using cartridge heaters and actively cooling the other side using a heat transfer fluid circulation system with a built-in temperature controller. Aluminum adapter plates transition from the heater and heat sink dimensions to the sample size (1 cm x 1 cm), and the high thermal conductivity of the aluminum creates approximately one-dimensional heat conduction in the specimen. The hot and the cold side temperatures are measured using surface thermocouples. An Infrared (IR) microscope with a spatial resolution of 1.8 μm and a temperature resolution of 0.1 K maps the steady state temperature distribution of the top surface of the specimen during thermal analysis. The experimental rig was designed to ensure one-dimensional thermal conduction in homogeneous material samples. The aluminum adapter plates, because of their high thermal conductivity, ensure that majority of the temperature drop occurs across the specimen. For heterogeneous materials, this

rig can be used to characterize an effective thermal conductivity in the direction of applied temperature gradient.

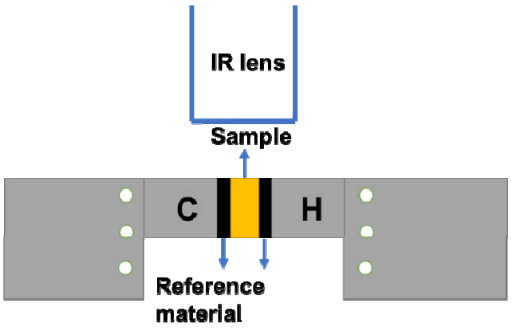

Fig. 2: Miniaturized IR reference bar measurement system sketch. The hot side (H) and cold side (C) adapter plates sandwich the specimen. Cartridge heater mounting holes are present on both adapter plates; these are used for heating the specimen to a constant temperature to measure emissivity. Thermal paste is applied at all interfaces to minimize interfacial temperature jumps. At steady state, the IR microscope measures the spatially varying temperature field.

Prior to measuring the steady-state temperature maps, the spatially varying emissivity of the specimen is calculated by heating the sample to a uniform, constant temperature. Surface thermocouples attached to the adapter plates, near the reference layers, monitor the temperature of the specimen. During calibration, the IR microscope software measures the radiative heat flux from the specimen and with the user-input surface temperature calculates the emissivity map. Given that the two reference layers are identical, comparing the emissivity in those regions is used as a verification that the system has reached a uniform temperature. Figure 3(a) shows the calculated emissivity map of the specimen during calibration. Although some uncertainty in temperature arises from uncertainty in the measured reference temperature during emissivity calibration, analysis of the results indicates that a ±0.5°C uncertainty in the reference temperature translates to a ±3% uncertainty in emissivity and <<1% uncertainty in thermal gradients within the sample. Non-uniform temperatures at the edges of the sample during calibration may lead to additional uncertainty in emissivity as indicated by the slightly lower emissivities at the edges of the sample, but the analysis of thermal conductivity is confined, in general, to the center portion of the sample with approximately uniform emissivity as shown in Fig. 3(b).

Because this work focuses on the effective thermal conductivity of the composite, the interface resistances between the composite sample and the references are minimized by using thermal paste between the reference layers and the sample. Black polytetrafluoroethylene (PTFE) layers serve as the reference when analyzing the neat epoxy (i.e., the polymer matrix) thermal conductivity, and fused silica is the reference for the higher conductivity composite materials. Table 1 shows the thermal conductivity of the reference materials that were characterized in-house.

Table 1. Reference materials and their thermal conductivities, as characterized in-house

#	Sample	Reference material	Thermal conductivity [W/m-K]
1	Neat epoxy	Polytetrafluoro-ethylene (PTFE)	0.3
2	Composite	Fused silica	1.4

The uniqueness of our measurement technique lies in (a) evaluation of thermal conductivity of the sample independent of contact resistances and (b) visualization of thermal conduction pathways in the sample. Investigating thermal conduction pathways in heterogeneous media is crucial to the processing of these materials for tailored properties. Thermal conduction in these composites is dictated by the morphology and topology of filler particles (i.e., graphite flakes). Correlating thermal conduction with microstructural characteristics of the composite, in addition to the topological arrangements of the filler particles, equips us with a tool to optimize materials processing conditions for the design of improved composite and thermal interface materials. Analyzing the arrangement of filler particles in the composite material (i.e., microstructural features such as interparticle connectivity and contact topology) coupled with particle morphological characteristics (such as the aspect ratio) is crucial to the evaluation of processing conditions and parameters.

ANALYSIS OF TEMPERATURE MAPS

To analyze thermal conduction in the samples, steady state temperature maps of the specimen top surface are analyzed. Heat transfer in this system is truly 3D, but in a region near the centerline of the sample, it can be approximated as 1D and simply analyzed with Fourier's Law. The average heat flux in the system (q'') is measured from the heat fluxes in the reference layers. The thermal conductivity of the reference layers, k_{ref}, is known; the temperature gradient in the reference layers, $\frac{dT}{dx_{ref}}$, is measured by the slope of best fit linear profiles to the temperature profile. By Fourier's Law, the product of these two quantities is the heat flux in the reference layer. The discrepancy in measured heat fluxes (reported below as percent of nominal measured heat flux in the system) in the reference layers accounts, in part, for convection heat losses and corresponds to the true multi-dimensional nature of heat conduction across the specimen. The mean difference in measured reference layer heat fluxes with the neat epoxy specimen is approximately 8.64%. However, for the composite material, approximately the entire width of the reference layers was analyzed. For the composite sample with 25% volume fraction of filler particles, this mean difference is 19.47%; this manifests as uncertainty in measured effective thermal conductivity (±0.5 W/m-K, see Figure 6(b)). Given that thermal conductivity of the filler particles is orders of magnitude larger than matrix

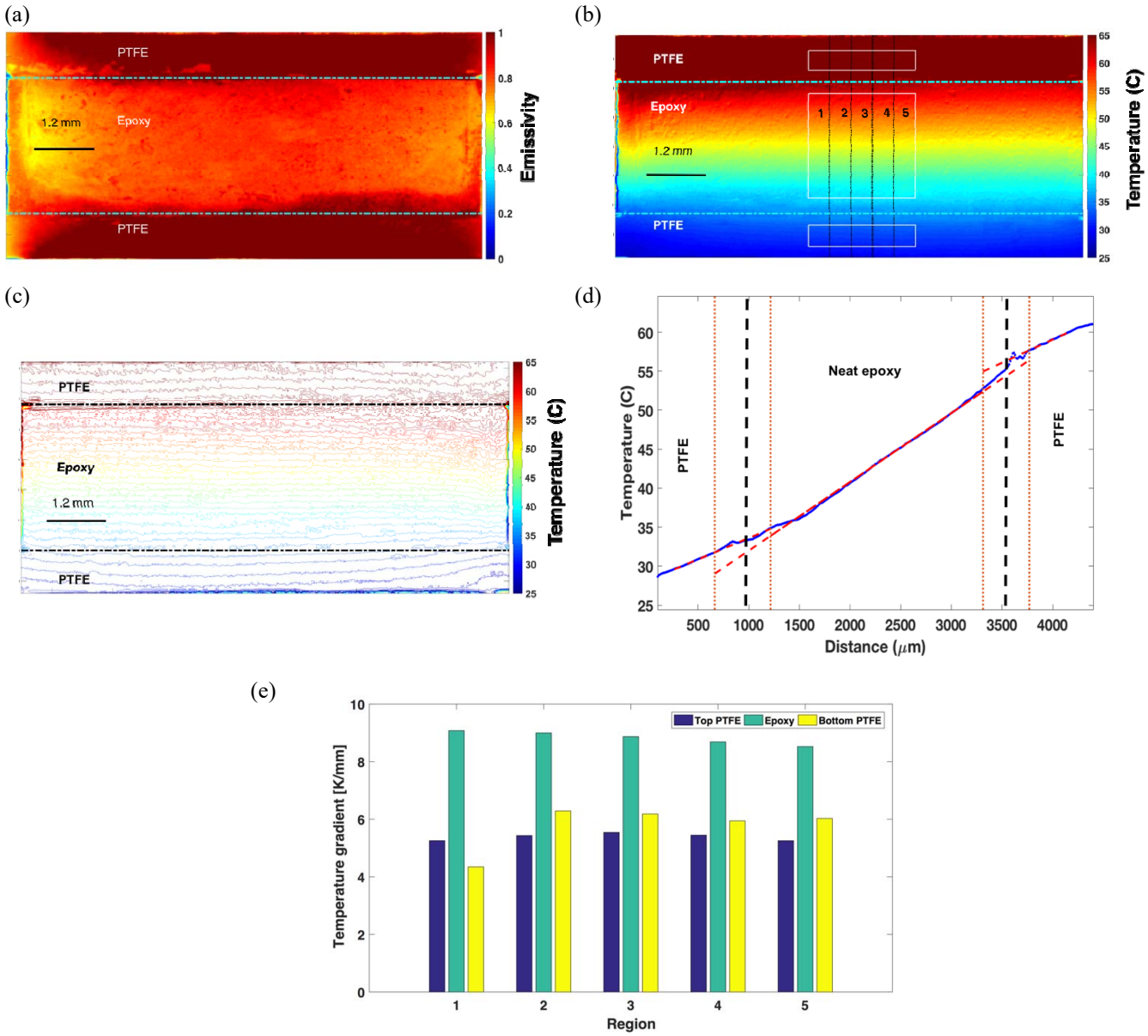

Fig. 3: (a) Emissivity map of the PTFE-epoxy-PTFE specimen. (b) Temperature map of the specimen showing the rectangular region of interest which is further divided into five regions for investigating thermal gradient variations. (c) Isothermal contours in the entire domain showing reasonably 1D heat flow near the center of the domain. (d) Corresponding 1D temperature profile when the temperature in each row of pixels is averaged. Linear temperature profiles are clearly observed in the sample and reference regions, and best fit linear profiles are indicated with red dashed lines. (e) Thermal gradients for the reference and sample regions within each sub-region of interest (see panel (b)). The consistent gradients in each region for the sample indicates the 1D approximation is reasonable in the center of the sample.

conductivity, variation in the measured reference layer heat fluxes is also an indicator of microstructural anisotropy of the composite (*i.e.*, high degree of microstructural alignment promotes 1D heat flow).

Qualitatively, from the temperature map, the isotherms are reasonably parallel, except near the edges (see Figure 3(c)). Thus, a region of interest is selected where the heat transfer is approximately one-dimensional (see Figure 3(b)), and the average temperature along the direction perpendicular to the dominant heat flow direction is calculated (see Figure 3(d)) to analyze the heat transfer rate and effective thermal conductivity. Theoretically, at steady state, the temperature profile in each homogenous material should be linear. Thus, a linear profile is fit to the portions of the temperature distribution corresponding to each reference and the sample regions. To confirm the region selected is sufficiently small to assume 1D heat transfer, the selected region is divided into 5 regions (see Figure 3(b)), and the thermal gradient is analyzed independently in each region (see Figure 3(d)). The variation in thermal gradients between different regions is small for the homogeneous, neat epoxy sample. Thus, Fourier's law for one-dimensional heat conduction is used to compute the average heat flux in the system (for both neat epoxy and composites) using reference material thermal conductivity and

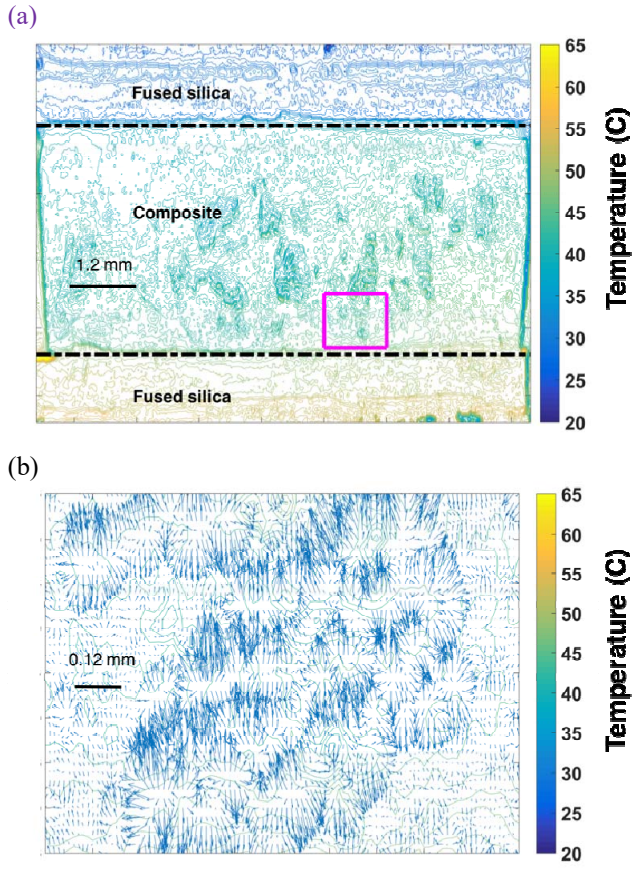

Fig. 4: (a) Isothermal contours at steady-state in a fused silica-composite-fused silica assembly. Clusters of contours represent the filler particles, *i.e.*, graphite flakes. (b) Heat flow lines reveal two-dimensional thermal pathways in a sub-section of the composite (*i.e.*, the orange box in (a)); clusters of arrows represent particulate regions.

temperature gradients in the respective reference regions. Finally, the thermal conductivity of the sample is extracted from the temperature gradient in this region and average of the hot and cold side heat fluxes.

RESULTS AND DISCUSSION

Heat conduction in the composites is multi-dimensional. Large variations of the thermal gradient in different rectangular regions are observed, as discussed below. Therefore, we define an effective temperature gradient across the sample in order to estimate an effective thermal conductivity:

$$\frac{dT}{dx} \approx \frac{\Delta T}{\Delta x_{eff,c}} \quad (1)$$

where ΔT is the total temperature drop across the sample and $\Delta x_{eff,c}$ is the effective composite thickness in the region analyzed (*i.e.*, away from interfacial effects). We calculate the effective thermal conductivity of the composite as

$$k_{eff} = \frac{q''}{\frac{\Delta T}{\Delta x}} \quad (2)$$

Emissivity maps for the composites show that emissivity of graphite particles significantly differs from the matrix (*i.e.*, epoxy) emissivity. Note that compared to work in the literature on nanocomposites, the filler particles here are

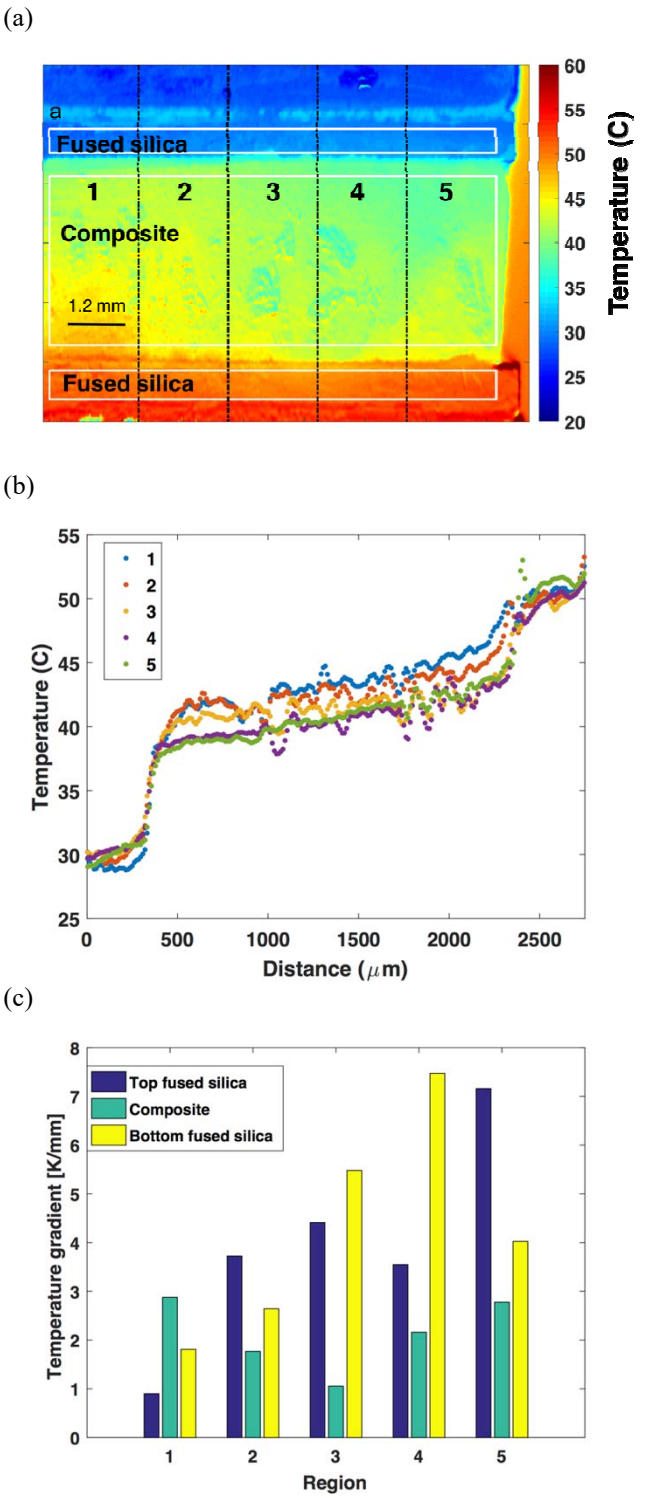

Fig. 5: (a) Temperature map for the composite sample illustrating the complete rectangular region of interest divided into 5 sub-regions regions to illustrate local temperature variation. White boxes define different regions (*i.e.*, fused silica-composite-fused silica); red dashed lines indicate interfaces. (b) Averaged "1D" temperature profile in each of the sub-regions. (c) Effective temperature gradients in each of the regions. Variations between the different regions highlight the two-dimensional nature of heat conduction in the composites.

relatively large compared to the thickness of the sample. Specifically, the particle diameter is only an order of magnitude smaller than the sample thickness. The isotherms also reveal that thermal conduction in the sample is two-dimensional. The gradient of temperature is computed to visualize heat flow lines in the composite. Clustering of contours (Figure 4(a)) and heat flow arrows (Figure 4(b)) correspond to the graphite flakes or filler particle phase.

A region of interest is selected to calculate an effective temperature gradient (see Figure 5(a)). The gradient along the vertical direction is greater than that along a horizontal direction in temperature map. The dominant heat flow pathway and the applied temperature gradient is in the vertical direction (Figure 4). But the quasi-one dimensional analysis for the composite thermal conductivity fails because the temperature gradient across the regions with filler particles is non-linear. This behavior is illustrated by the significant variation in local thermal gradients when the region of interest is subdivided into rectangular regions (Figure 5(c)). When compared with the variation in gradients in neat epoxy (Figure 3(e)), the impact of the filler material is clear. Local variations in temperature gradient, due to the presence of filler particles (*i.e.*, graphite flake) with orders of magnitude higher thermal conductivity than the matrix phase (*i.e.*, epoxy), are observed

(a)

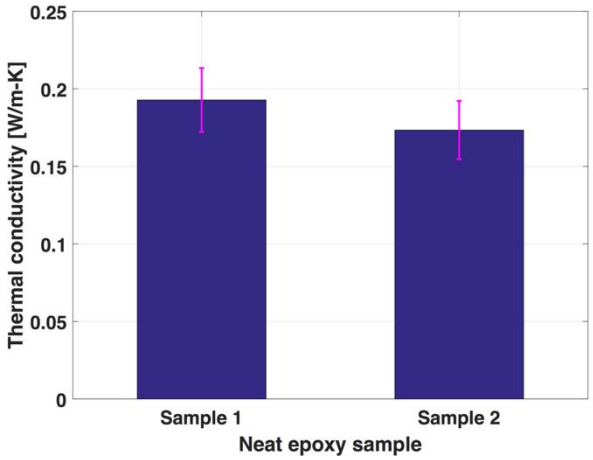

(b)

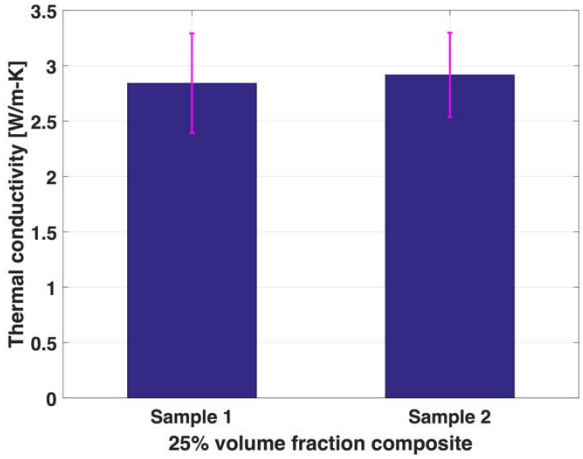

Fig. 6: Thermal conductivity of (a) neat epoxy and (b) composites with 25% filler volume fraction.

(Figure 5(b)). While these variations can be smoothed by averaging the data, doing so will add to uncertainty in the estimated thermal conductivity. Nevertheless, the two-dimensional nature of thermal conduction is of primary interest here. To the best of our knowledge, a direct observation of such heat flow pathways has not been reported in prior literature.

Error bars in our data for thermal conductivity are estimated from an uncertainty propagation approach. Uncertainty in the measured thermal conductivity of the epoxy and the composite derives from the uncertainties in the measured temperature gradient in the reference layer, which along with the thermal conductivity of the reference layers, is used to quantify the heat flux flowing across the system and in the measured temperature gradient in the sample. The uncertainty in reference material thermal conductivity is assumed to be 10% of its nominal value. The spatially varying emissivity in the specimen is based on a reference temperature, T_{ref}, which is measured using T-type thermocouples with an accuracy of ± 0.5 ℃ leading to an error in emissivity calibration of about $\pm 3\%$. However, our analytical calculations indicate that a 17% change in emissivity implies $< 4\%$ error in the absolute value of temperature, up to 350 K, and an even smaller uncertainty in the slope of the temperature (<1%). The uncertainty in calculated temperature gradient in the sample material region (*i.e.*, by manual selection of regions) is assumed to be independent of the uncertainty in the estimated heat flux.

To assess the thermal performance of the graphite flake-epoxy composites, we first characterize the thermal conductivity of the epoxy samples with black polytetrafluoroethylene as the reference layers. As mentioned earlier, the specimen emissivity is first calibrated by heating it to a nearly constant surface temperature (73℃ for both samples). Four measurements are performed at different applied power levels (*i.e.*, monotonically decreasing for successive thermal maps) to estimate the thermal conductivity of the epoxy. The estimated thermal conductivity of the neat epoxy is 0.18 W/m-K, and the results from two separate samples agree within 10% and within the uncertainty of the measurement. For the two separate samples of composite material with 25% filler particles, the nominal effective thermal conductivity is 2.9 W/m-K, and the results for two samples agree within 3%. Potentially, the minimal variation between the two composites could suggest that the arrangement of filler particles in the two composites is statistically similar.

CONCLUSIONS AND OUTLOOK

In summary, we demonstrate use of IR microscopy to (a) characterize thermal conductivity of graphite flake-epoxy thermal interface materials (TIMs) and (b) visualize spatially varying temperature distribution in these materials. The neat epoxy is isotropic and homogenous, but the composite is heterogeneous, as indicated by the non-uniform spatial distribution of particles in the composite, resulting in a non-uniform thermal conductivity. We observed a 16-fold enhancement in the effective thermal conductivity of the composite relative to the neat epoxy at 25% volume fraction. Processing techniques specifically focused on uniform

dispersion of filler particles in TIMs and preferential alignment of these filler particles may further enhance the composite thermal conductivity. This study forms the basis for future investigation of shear-induced alignment [18] of platelet-like graphitic particles, control of viscosity of the polymer, and contributes towards the development of processing methods, such as rheological processing of polymeric suspensions, to fabricate materials with tailored thermal properties for application in electronics heat dissipation. Moreover, particle shape and aspect ratio have also been reported to impact thermal conductivity of TIMs and this technique can be used to interrogate materials with a variety of filler particle geometries. Additionally, while in the literature, percolation has been inferred to be the cause of abrupt increases in thermal conductivity, a direct correlation between microstructure, percolation, and thermal conduction pathways has not yet been demonstrated. By combining the method developed here with transient temperature imaging, the impact of alignment of filler particles in the composite should reveal more information about percolation.

Acknowledgments

The authors thank Asbury Carbons for providing us with free samples of the graphite flakes used in this study as well as SEM images of the individual flakes and particle size distribution.

References

1. G. Lian, C. C. Tuan, L. Li et al. "Vertically Aligned and Interconnected Graphene Networks for High Thermal Conductivity of Epoxy Composites with Ultralow Loading", Chem. Mater., Vol. 28, pp. 6096−6104, August 2016.
2. X. Shen, Z. Wang, Y. Wu et al. "Multilayer Graphene Enables Higher Efficiency in Improving Thermal Conductivities of Graphene/Epoxy Composites", Nano Lett., Vol. 16, pp. 3585−3593, May 2016.
3. M. Shtein, R. Nadiv, M. Buzaglo et al. "Thermally Conductive Graphene-Polymer Composites: Size, Percolation, and Synergy Effect", Chem. Mater., Vol. 27, pp. 2100−2106, Feb 2015.
4. Y. Sun, B. Tang, W. Huang et al. "Preparation of graphene modified epoxy resin with high thermal conductivity by optimizing the morphology of filler", Applied Thermal Engineering Vol. 103, pp. 892–900, May 2016.
5. M. Sharifi, C. Jang, C. F. Abrams, et al. “Epoxy Polymer Networks with Improved Thermal and Mechanical Properties via Controlled Dispersion of Reactive Toughening Agents”, Macromolecules, 48, pp. 7495−7502, Oct 2015.
6. A. A. Balandin, S. Ghosh, W. Bao et al. “Superior Thermal Conductivity of Single-Layer Graphene”, Nano Letters, Vol. 8, No. 3, pp. 902-907, Jan 2008.
7. H. S. Kim, H. S. Bae, J. Yu et al. “Thermal conductivity of polymer composites with the geometrical characteristics of graphene nanoplatelets”, Scientific Reports, 6, 26825, May 2016.
8. S. Y. Kim, Y. J. Noh, J. Yu, “Thermal conductivity of graphene nanoplatelets filled composites fabricated by solvent-free processing for the excellent filler dispersion and a theoretical approach for the composites containing the geometrized fillers”, Composites: Part A, Vol. 69, pp. 219–225, Nov 2014.
9. A. Yu, P. Ramesh, M. E. Itkis, et al.“Graphite nanoplatelet-epoxy composite thermal interface materials”, The Journal of Physical Chemistry C, Vol. 111, pp. 7565-7569, April 2007.
10. S. Kale, F. A. Sabet, I. Jasiuk, and M. Ostoja-Starzewski, “Effect of filler alignment on percolation in polymer nanocomposites using tunneling-percolation model,” *J. Appl. Phys.*, vol. 120, no. 4, p. 45105, 2016.
11. B. Dan, B. G. Sammakia, G. Subbarayan, S. Kanuparthi, and S. Mallampati, “The study of the polydispersivity effect on the thermal conductivity of particulate thermal interface materials by finite element method,” *IEEE Trans. Components, Packag. Manuf. Technol.*, vol. 3, no. 12, pp. 2068–2074, 2013.
12. Y. B. Yi and E. Tawerghi, “Geometric percolation thresholds of interpenetrating plates in three-dimensional space,” *Phys. Rev. E - Stat. Nonlinear, Soft Matter Phys.*, vol. 79, no. 4, pp. 1–6, 2009.
13. H. LI, S. KAIRA, J. MERTENS, N. CHAWLA, and Y. JIAO, “Accurate stochastic reconstruction of heterogeneous microstructures by limited x-ray tomographic projections,” *J. Microsc.*, vol. 264, no. 3, pp. 339–350, 2016.
14. Y. Jiao and N. Chawla, “Three dimensional modeling of complex heterogeneous materials via statistical microstructural descriptors,” *Integr. Mater. Manuf. Innov.*, vol. 3, no. 1, p. 3, 2014.
15. “Standard Test Method for Thermal Transmission Properties of Thermally Conductive Electrical Insulation Materials”, ASTM D5470-12, American Society for Testing and Materials, Feb 2012.
16. A. Gaitonde, A. Marconnet, and A. Nimmagadda, “Measurement of interfacial thermal conductance in Li-ion batteries,” *J. Power Sources*, vol. 343, pp. 431–436, 2017.
17. A. M. Marconnet, M. a. Panzer, and K. E. Goodson, “Thermal conduction phenomena in carbon nanotubes and related nanostructured materials,” *Rev. Mod. Phys.*, vol. 85, no. 3, pp. 1295–1326, 2013.
18. L. Gan, F. Qiu, Y. Hao, K. Zhang, Z. Zhou, J. Zeng, and M. Wang, “Shear-induced orientation of functional graphene oxide sheets in isotactic polypropylene,” pp. 5185–5195, 2016.